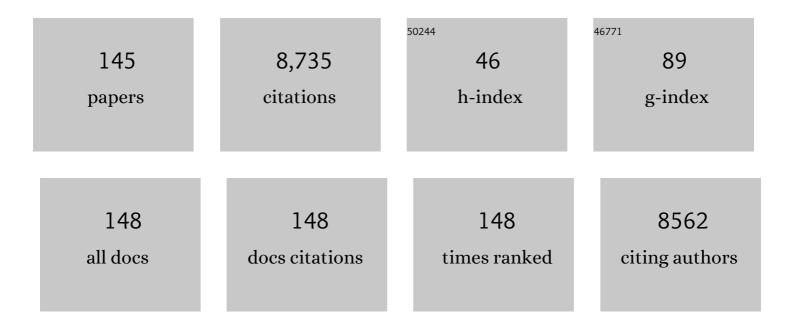
Wenjing Tian

List of Publications by Year in descending order

Source: https://exaly.com/author-pdf/366968/publications.pdf Version: 2024-02-01



#	Article	IF	CITATIONS
1	Piezochromic Luminescence Based on the Molecular Aggregation of 9,10â€Bis((<i>E</i>)â€2â€{pyridâ€2â€yl)vinyl)anthracene. Angewandte Chemie - International Edition, 2012, 51, 10782-10785.	7.2	787
2	Low-temperature SnO ₂ -based electron selective contact for efficient and stable perovskite solar cells. Journal of Materials Chemistry A, 2015, 3, 10837-10844.	5.2	324
3	Solid-State Photoinduced Luminescence Switch for Advanced Anticounterfeiting and Super-Resolution Imaging Applications. Journal of the American Chemical Society, 2017, 139, 16036-16039.	6.6	323
4	Remarkable Turnâ€On and Colorâ€Tuned Piezochromic Luminescence: Mechanically Switching Intramolecular Charge Transfer in Molecular Crystals. Advanced Functional Materials, 2015, 25, 4005-4010.	7.8	308
5	Aggregation-Induced Emission in the Crystals of 9,10-Distyrylanthracene Derivatives: The Essential Role of Restricted Intramolecular Torsion. Journal of Physical Chemistry C, 2009, 113, 9892-9899.	1.5	283
6	Organic Polymorphs: Oneâ€Compoundâ€Based Crystals with Molecularâ€Conformation―and Packingâ€Dependent Luminescent Properties. Advanced Materials, 2014, 26, 6168-6173.	11.1	262
7	Highly Efficient Far Red/Nearâ€Infrared Solid Fluorophores: Aggregationâ€Induced Emission, Intramolecular Charge Transfer, Twisted Molecular Conformation, and Bioimaging Applications. Angewandte Chemie - International Edition, 2016, 55, 155-159.	7.2	257
8	AlEgen with Fluorescence–Phosphorescence Dual Mechanoluminescence at Room Temperature. Angewandte Chemie - International Edition, 2017, 56, 880-884.	7.2	250
9	Fluorescent nanoparticles based on AIE fluorogens for bioimaging. Nanoscale, 2016, 8, 2471-2487.	2.8	236
10	Solution processable $D\hat{a}\in$ "A small molecules for bulk-heterojunction solar cells. Energy and Environmental Science, 2010, 3, 1427.	15.6	225
11	Multi-stimuli responsive fluorescence switching: the reversible piezochromism and protonation effect of a divinylanthracene derivative. Journal of Materials Chemistry C, 2013, 1, 7554.	2.7	197
12	Piezochromic Luminescence of Donor–Acceptor Cocrystals: Distinct Responses to Anisotropic Grinding and Isotropic Compression. Angewandte Chemie - International Edition, 2018, 57, 15670-15674.	7.2	172
13	An AIE-active luminophore with tunable and remarkable fluorescence switching based on the piezo and protonation–deprotonation control. Chemical Communications, 2014, 50, 7374-7377.	2.2	161
14	Self-assembled graphene quantum dots induced by cytochrome c: a novel biosensor for trypsin with remarkable fluorescence enhancement. Nanoscale, 2013, 5, 7776.	2.8	142
15	An Organic Luminescent Molecule: What Will Happen When the "Butterflies―Come Together?. Advanced Materials, 2014, 26, 739-745.	11.1	142
16	Mechanochromism and Polymorphism-Dependent Emission of Tetrakis(4-(dimethylamino)phenyl)ethylene. Journal of Physical Chemistry C, 2013, 117, 24997-25003.	1.5	140
17	Folic acid-functionalized mesoporous silica nanospheres hybridized with AIE luminogens for targeted cancer cell imaging. Nanoscale, 2013, 5, 2065.	2.8	133
18	Organic molecular aggregates: From aggregation structure to emission property. Aggregate, 2021, 2, e96.	5.2	131

#	Article	IF	CITATIONS
19	Low-temperature-processed ZnO–SnO2 nanocomposite for efficient planar perovskite solar cells. Solar Energy Materials and Solar Cells, 2016, 144, 623-630.	3.0	129
20	Remarkable fluorescence change based on the protonation–deprotonation control in organic crystals. Chemical Communications, 2013, 49, 3878.	2.2	111
21	AIE (AIEE) and mechanofluorochromic performances of TPE-methoxylates: effects of single molecular conformations. RSC Advances, 2013, 3, 7996.	1.7	108
22	Reversible Luminescent Switching in an Organic Cocrystal: Multiâ€Stimuliâ€Induced Crystalâ€toâ€Crystal Phase Transformation. Angewandte Chemie - International Edition, 2020, 59, 15098-15103.	7.2	100
23	Fluorescent Aptasensor Based on Aggregation-Induced Emission Probe and Graphene Oxide. Analytical Chemistry, 2014, 86, 298-303.	3.2	92
24	AlEgen with Fluorescence–Phosphorescence Dual Mechanoluminescence at Room Temperature. Angewandte Chemie, 2017, 129, 898-902.	1.6	90
25	Organic Laser Molecule with High Mobility, High Photoluminescence Quantum Yield, and Deep-Blue Lasing Characteristics. Journal of the American Chemical Society, 2020, 142, 6332-6339.	6.6	90
26	Aggregation emission properties and self-assembly of conjugated oligocarbazoles. Chemical Communications, 2011, 47, 6602.	2.2	88
27	Oligo(phenothiazine)s: Twisted Intramolecular Charge Transfer and Aggregation-Induced Emission. Journal of Physical Chemistry C, 2013, 117, 23117-23125.	1.5	86
28	Reversible Multistimuliâ€Response Fluorescent Switch Based on Tetraphenylethene–Spiropyran Molecules. Chemistry - A European Journal, 2015, 21, 1149-1155.	1.7	86
29	Highly efficient and stable low-temperature processed ZnO solar cells with triple cation perovskite absorber. Journal of Materials Chemistry A, 2017, 5, 13439-13447.	5.2	86
30	Tunable Supramolecular Interactions of Aggregationâ€Induced Emission Probe and Graphene Oxide with Biomolecules: An Approach toward Ultrasensitive Labelâ€Free and "Turnâ€On―DNA Sensing. Small, 2016, 3 6613-6622.	12,5.2	75
31	Magnesiumâ€doped Zinc Oxide as Electron Selective Contact Layers for Efficient Perovskite Solar Cells. ChemSusChem, 2016, 9, 2640-2647.	3.6	74
32	Efficient Bulk-Heterojunction Solar Cells Based on a Symmetrical D-ï€-A-ï€-D Organic Dye Molecule. Journal of Physical Chemistry C, 2009, 113, 12911-12917.	1.5	73
33	Synthesis of 4,7-Diphenyl-2,1,3-Benzothiadiazole-Based Copolymers and Their Photovoltaic Applications. Macromolecules, 2009, 42, 4977-4984.	2.2	72
34	Efficient and Environmentally Stable Perovskite Solar Cells Based on ZnO Electron Collection Layer. Chemistry Letters, 2015, 44, 610-612.	0.7	72
35	HC(NH ₂) ₂ PbI ₃ as a thermally stable absorber for efficient ZnO-based perovskite solar cells. Journal of Materials Chemistry A, 2016, 4, 8435-8443.	5.2	72
36	Using fluorine-containing amphiphilic random copolymers to manipulate the quantum yields of aggregation-induced emission fluorophores in aqueous solutions and the use of these polymers for fluorescent bioimaging. Journal of Materials Chemistry, 2012, 22, 9890.	6.7	71

#	Article	IF	CITATIONS
37	Organic UVâ€5ensitive Phototransistors Based on Distriphenylamineethynylpyrene Derivatives with Ultraâ€High Detectivity Approaching 10 ¹⁸ . Advanced Materials, 2020, 32, e1907791.	11.1	71
38	TICT-Based Near-Infrared Ratiometric Organic Fluorescent Thermometer for Intracellular Temperature Sensing. ACS Applied Materials & amp; Interfaces, 2020, 12, 26842-26851.	4.0	70
39	A label-free aptasensor for turn-on fluorescent detection of ATP based on AIE-active probe and water-soluble carbon nanotubes. Sensors and Actuators B: Chemical, 2016, 230, 556-558.	4.0	63
40	Label-Free Aptamer-Based Biosensor for Specific Detection of Chloramphenicol Using AIE Probe and Graphene Oxide. ACS Omega, 2018, 3, 12886-12892.	1.6	60
41	Supramolecular Hybrids of AlEgen with Carbon Dots for Noninvasive Long-Term Bioimaging. Chemistry of Materials, 2016, 28, 8825-8833.	3.2	59
42	Efficient polymer/nanocrystal hybrid solar cells fabricated from aqueous materials. Energy and Environmental Science, 2011, 4, 2831.	15.6	58
43	Folic acid-functionalized AIE Pdots based on amphiphilic PCL-b-PEG for targeted cell imaging. Polymer Chemistry, 2014, 5, 3824-3830.	1.9	56
44	A highly sensitive "turn-on―fluorescent probe for bovine serum albumin protein detection and quantification based on AlE-active distyrylanthracene derivative. Science China Chemistry, 2013, 56, 1234-1238.	4.2	55
45	"Turn-on―Fluorescent Aptasensor Based on AlEgen Labeling for the Localization of IFN-γ in Live Cells. ACS Sensors, 2018, 3, 320-326.	4.0	53
46	Ultra bright red AIE dots for cytoplasm and nuclear imaging. Polymer Chemistry, 2014, 5, 7013-7020.	1.9	50
47	Integrating Efficient Optical Gain in Highâ€Mobility Organic Semiconductors for Multifunctional Optoelectronic Applications. Advanced Functional Materials, 2018, 28, 1802454.	7.8	50
48	Insights into the origin of aggregation enhanced emission of 9,10-distyrylanthracene derivatives. Materials Chemistry Frontiers, 2017, 1, 1422-1429.	3.2	47
49	A TPE-oxazoline molecular switch with tunable multi-emission in both solution and solid state. RSC Advances, 2013, 3, 16986.	1.7	46
50	Luminescent switching and structural transition through multiple external stimuli based on organic molecular polymorphs. Journal of Materials Chemistry C, 2019, 7, 3263-3268.	2.7	44
51	A theoretical study of hybrid lead iodide perovskite homologous semiconductors with 0D, 1D, 2D and 3D structures. Journal of Materials Chemistry A, 2017, 5, 16786-16795.	5.2	43
52	Label-free fluorescence turn-on detection of Pb ²⁺ based on AIE-active quaternary ammonium salt of 9,10-distyrylanthracene. Analytical Methods, 2013, 5, 438-441.	1.3	42
53	Dual-functional two-dimensional covalent organic frameworks for water sensing and harvesting. Materials Chemistry Frontiers, 2021, 5, 4193-4201.	3.2	41
54	Tetraphenylethylene-Based Emissive Supramolecular Metallacages Assembled by Terpyridine Ligands. CCS Chemistry, 2020, 2, 337-348.	4.6	39

#	Article	IF	CITATIONS
55	Proton-Triggered Hypsochromic Luminescence in 1,1′-(2,5-Distyryl-1,4-phenylene) Dipiperidine. Journal of Physical Chemistry Letters, 2014, 5, 2781-2784.	2.1	38
56	Morphology controllable conjugated network polymers based on AIE-active building block for TNP detection. Chinese Chemical Letters, 2021, 32, 1037-1040.	4.8	38
57	Synthesis of a Waterâ€Soluble Conjugated Polymer Based on Thiophene for an Aqueousâ€Processed Hybrid Photovoltaic and Photodetector Device. Advanced Materials, 2014, 26, 3655-3661.	11.1	35
58	A sensitive and selective "turn-on―fluorescent probe for Hg ²⁺ based on thymine–Hg ²⁺ –thymine complex with an aggregation-induced emission feature. Analytical Methods, 2014, 6, 2338-2342.	1.3	34
59	Direct Observation of the Symmetrical and Asymmetrical Protonation States in Molecular Crystals. Journal of Physical Chemistry Letters, 2017, 8, 3068-3072.	2.1	32
60	Tailoring the morphology of AlEgen fluorescent nanoparticles for optimal cellular uptake and imaging efficacy. Chemical Science, 2018, 9, 2620-2627.	3.7	32
61	Rhodamine-naphthalimide demonstrated a distinct aggregation-induced emission mechanism: elimination of dark-states <i>via</i> dimer interactions (EDDI). Chemical Communications, 2019, 55, 1446-1449.	2.2	32
62	Donor–acceptor copolymers incorporating polybenzo[1,2-b:4,5-b′]dithiophene and tetrazine for high open circuit voltage polymer solar cells. Organic Electronics, 2013, 14, 2124-2131.	1.4	31
63	Organic dye doped nanoparticles with NIR emission and biocompatibility for ultra-deep inÂvivo two-photon microscopy under 1040ÂnmÂfemtosecond excitation. Dyes and Pigments, 2017, 143, 76-85.	2.0	31
64	Turn-on sensing for Ag+ based on AIE-active fluorescent probe and cytosine-rich DNA. Analytical and Bioanalytical Chemistry, 2015, 407, 2625-2630.	1.9	30
65	Highly efficient Far Red/Near-Infrared fluorophores with aggregation-induced emission for bioimaging. Dyes and Pigments, 2017, 142, 491-498.	2.0	30
66	Low-Loss Optical Waveguide and Highly Polarized Emission in a Uniaxially Oriented Molecular Crystal Based on 9,10-Distyrylanthracene Derivatives. ACS Photonics, 2015, 2, 313-318.	3.2	29
67	Silica nanoparticles based on an AIE-active molecule for ratiometric detection of RNS <i>in vitro</i> . Journal of Materials Chemistry B, 2017, 5, 9197-9203.	2.9	29
68	Influence of hole transport layers on internal absorption, charge recombination and collection in HC(NH ₂) ₂ PbI ₃ perovskite solar cells. Journal of Materials Chemistry A, 2018, 6, 7922-7932.	5.2	29
69	Covalent Organic Frameworks with Electronâ€Rich and Electronâ€Deficient Structures as Water Sensing Scaffolds. Macromolecular Rapid Communications, 2020, 41, e2000003.	2.0	29
70	Polymorphism-Dependent Enhanced Emission in Molecular Aggregates: J-Aggregate versus X-Aggregate. Journal of Physical Chemistry Letters, 2020, 11, 10504-10510.	2.1	29
71	Organic Single Crystals with High Photoluminescence Quantum Yields Close to 100% and High Mobility for Optoelectronic Devices. Advanced Materials, 2021, 33, e2105466.	11.1	29
72	Synthesis, photophysical and photovoltaic properties of star-shaped molecules with triphenylamine as core and phenylethenylthiophene or dithienylethylene as arms. Solar Energy Materials and Solar Cells, 2009, 93, 1952-1958.	3.0	28

#	Article	IF	CITATIONS
73	Recent Advances in Mechanism of AIE Mechanochromic Materials. Chemical Research in Chinese Universities, 2021, 37, 100-109.	1.3	27
74	Reversible Threeâ€Color Fluorescence Switching of an Organic Molecule in the Solid State via "Pump–Trigger―Optical Manipulation. Angewandte Chemie - International Edition, 2022, 61, .	7.2	27
75	Highly efficient near-infrared organic dots based on novel AEE fluorogen for specific cancer cell imaging. RSC Advances, 2015, 5, 36837-36844.	1.7	26
76	High-Efficiency Aqueous-Solution-Processed Hybrid Solar Cells Based on P3HT Dots and CdTe Nanocrystals. ACS Applied Materials & Interfaces, 2015, 7, 7146-7152.	4.0	26
77	Effect of ZnO Electron Extraction Layer on Charge Recombination and Collection Properties in Organic Solar Cells. ACS Applied Energy Materials, 2019, 2, 7385-7392.	2.5	26
78	Label-free bioassay with graphene oxide-based fluorescent aptasensors: A review. Analytica Chimica Acta, 2021, 1188, 338859.	2.6	26
79	Organic polymorphs with fluorescence switching: direct evidence for mechanical and thermal modulation of excited state transitions. Chemical Communications, 2019, 55, 3749-3752.	2.2	25
80	Self-assembled nanostructured photosensitizer with aggregation-induced emission for enhanced photodynamic anticancer therapy. Science China Materials, 2020, 63, 136-146.	3.5	25
81	A double hole-transport layer strategy toward efficient mixed tin-lead iodide perovskite solar cell. Solar Energy Materials and Solar Cells, 2020, 207, 110351.	3.0	25
82	Solid-State Reversible Dual Fluorescent Switches for Multimodality Optical Memory. Journal of Physical Chemistry Letters, 2021, 12, 1290-1294.	2.1	25
83	Imidazole-containing cyanostilbene-based molecules with aggregation-induced emission characteristics: photophysical and electroluminescent properties. New Journal of Chemistry, 2019, 43, 1844-1850.	1.4	24
84	Fulgide Derivative-Based Solid-State Reversible Fluorescent Switches for Advanced Optical Memory. CCS Chemistry, 2022, 4, 132-140.	4.6	24
85	Reversible Photoswitching between Fluorescence and Room Temperature Phosphorescence by Manipulating Excited State Dynamics in Molecular Aggregates. Angewandte Chemie - International Edition, 2022, 61, .	7.2	24
86	High-efficiency fluorescent and magnetic multimodal probe for long-term monitoring and deep penetration imaging of tumors. Journal of Materials Chemistry B, 2019, 7, 5345-5351.	2.9	22
87	Engineering Ultra Long Charge Carrier Lifetimes in Organic Electronic Devices at Room Temperature. Advanced Materials Interfaces, 2015, 2, 1400555.	1.9	21
88	Efficient Spontaneous and Stimulated Emission from 1,4â€Bis(2,2â€diphenylvinyl)benzene Single Crystals with Crossâ€Dipole Stacking. Advanced Optical Materials, 2015, 3, 763-768.	3.6	21
89	Intracellular pH sensing using polymeric micelle containing tetraphenylethylene-oxazolidine. Polymer Chemistry, 2016, 7, 5273-5280.	1.9	21
90	A Label-free Fluorescent Aptasensor for Turn-on Monitoring Ochratoxin A Based on AIE-active Probe and Graphene Oxide. Chemical Research in Chinese Universities, 2018, 34, 363-368.	1.3	21

Wenjing Tian

#	Article	IF	CITATIONS
91	Aggregation-induced emission of a 2D protein supramolecular nanofilm with emergent functions. Materials Chemistry Frontiers, 2020, 4, 1256-1267.	3.2	21
92	Aqueous-solution-processed PPV–CdxHg1â^'xTe hybrid solar cells with a significant near-infrared contribution. Journal of Materials Chemistry, 2012, 22, 17827.	6.7	20
93	Measuring electron and hole mobilities in organic systems: charge selective CELIV. Synthetic Metals, 2015, 203, 187-191.	2.1	20
94	Covalent organic hollow nanospheres constructed by using AIE-active units for nitrophenol explosives detection. Science China Chemistry, 2020, 63, 497-503.	4.2	20
95	Optical Waveguide and Photoluminescent Polarization in Organic Cocrystal Polymorphs. Journal of Physical Chemistry Letters, 2021, 12, 9233-9238.	2.1	20
96	Predicted Formation of H ₃ ⁺ in Solid Halogen Polyhydrides at High Pressures. Journal of Physical Chemistry A, 2015, 119, 11059-11065.	1.1	19
97	Combining plasmonic trap filling and optical backscattering for highly efficient third generation solar cells. Journal of Materials Chemistry A, 2017, 5, 3995-4002.	5.2	19
98	Reducing Photovoltage Loss in Inverted Perovskite Solar Cells by Quantum Dots Alloying Modification at Cathode Contact. Solar Rrl, 2020, 4, 1900468.	3.1	19
99	Construction and function of a highly efficient supramolecular luminescent system. Faraday Discussions, 2017, 196, 219-229.	1.6	17
100	Exploiting radical-pair intersystem crossing for maximizing singlet oxygen quantum yields in pure organic fluorescent photosensitizers. Chemical Science, 2020, 11, 10921-10927.	3.7	17
101	Achieving high open-circuit voltage in the PPV-CdHgTe bilayer photovoltaic devices on the basis of the heterojunction interfacial modification. Journal of Materials Chemistry, 2012, 22, 9161.	6.7	16
102	Highly sensitive determination of ssDNA and real-time sensing of nuclease activity and inhibition based on the controlled self-assembly of a 9,10-distyrylanthracene probe. Analytical and Bioanalytical Chemistry, 2014, 406, 851-858.	1.9	16
103	Redoxâ€responsive Fluorescent Nanoparticles Based on Diselenideâ€containing AlEgens for Cell Imaging and Selective Cancer Therapy. Chemistry - an Asian Journal, 2019, 14, 1745-1753.	1.7	16
104	Twisted Intramolecular Charge Transfer—Aggregation-Induced Emission Fluorogen with Polymer Encapsulation-Enhanced Near-Infrared Emission for Bioimaging. CCS Chemistry, 2021, 3, 2084-2094.	4.6	16
105	Low molecular mass organogel from mesomorphic Nâ€(4â€hexyloxybenzoyl)â€N′â€(4′â€nitrobenzoyl)hydra Liquid Crystals, 2006, 33, 439-443.	azine.	15
106	Observation of intercalated smectic phases in symmetric liquid crystal dimers containing hydrazide groups. Liquid Crystals, 2006, 33, 445-450.	0.9	14
107	Polyelectrolyte interlayers with a broad processing window for high efficiency inverted organic solar cells towards mass production. Journal of Materials Chemistry A, 2018, 6, 17662-17670.	5.2	13
108	Constructing Artificial Lightâ€Harvesting Systems by Covalent Alignment of Aggregationâ€Induced Emission Molecules. Macromolecular Rapid Communications, 2019, 40, 1800892.	2.0	13

#	Article	IF	CITATIONS
109	Co-assembly of HPV capsid proteins and aggregation-induced emission fluorogens for improved cell imaging. Nanoscale, 2020, 12, 5501-5506.	2.8	13
110	A two-step method combining electrodepositing and spin-coating for solar cell processing. Journal of Solid State Electrochemistry, 2010, 14, 1051-1056.	1.2	12
111	Acid Stimuli Responsive CPL from Supramolecular Assembly of AIE Molecule. Journal of Physical Chemistry C, 2021, 125, 21270-21276.	1.5	12
112	Organic semiconductors with a charge carrier life time of over 2 hours at room temperature. Journal of Materials Chemistry C, 2015, 3, 12260-12266.	2.7	11
113	Pressure-induced remarkable luminescence-changing behaviours of 9, 10-distyrylanthracene and its derivatives with distinct substituents. Dyes and Pigments, 2019, 161, 182-187.	2.0	11
114	Precise Detection and Visualization of Cyclooxygenase-2 for Golgi Imaging by a Light-Up Aggregation-Induced Emission-Based Probe. CCS Chemistry, 2022, 4, 456-463.	4.6	11
115	Deep-Red and Near-Infrared Iridium Complexes with Fine-Tuned Emission Colors by Adjusting Trifluoromethyl Substitution on Cyclometalated Ligands Combined with Matched Ancillary Ligands for Highly Efficient Phosphorescent Organic Light-Emitting Diodes. Molecules, 2022, 27, 286.	1.7	11
116	A covalent organic polymer for turn-on fluorescence sensing of hydrazine. Journal of Materials Chemistry C, 2022, 10, 2807-2813.	2.7	11
117	Electrochemistry and Electrogenerated Chemiluminescence of (dppy)BTPAa Bipolar, Solvatochromic Boron Compound. Journal of Physical Chemistry C, 2007, 111, 16345-16350.	1.5	10
118	Trap-limited bimolecular recombination in poly(3-hexylthiophene): Fullerene blend films. Organic Electronics, 2016, 38, 8-14.	1.4	10
119	Influence of organic cations on intrinsic properties of lead iodide perovskite solar cells. Organic Electronics, 2018, 62, 269-276.	1.4	10
120	Efficiency of MAPbI ₃ -Based Planar Solar Cell Analyzed by Its Thickness-Dependent Exciton Formation, Morphology, and Crystallinity. ACS Applied Materials & Interfaces, 2019, 11, 14810-14820.	4.0	10
121	Effects of DIO on the charge recombination behaviors of PTB7:PC71BM photovoltaics. Organic Electronics, 2019, 67, 50-56.	1.4	10
122	Fluorescent nanorods based on 9,10-distyrylanthracene (DSA) derivatives for efficient and long-term bioimaging. Journal of Materials Chemistry B, 2020, 8, 9544-9554.	2.9	10
123	Direct observation of intramolecular coplanarity regulated polymorph emission of a tetraphenylethene derivative. Chinese Chemical Letters, 2020, 31, 2985-2987.	4.8	10
124	Solution-processable two-dimensional conjugated organic small molecules containing triphenylamine cores for photovoltaic application. New Journal of Chemistry, 2014, 38, 5009-5017.	1.4	7
125	Pick and Place Distributed Feedback Lasers Using Organic Single Crystals. Advanced Optical Materials, 2020, 8, 1901785.	3.6	7
126	Molecular crystals based on 9,10-distyrylanthracene derivatives with high solid state fluorescence efficiency and uniaxial orientation induced by supramolecular interactions. Science Bulletin, 2013, 58, 2747-2752.	1.7	6

#	Article	IF	CITATIONS
127	Polymer grafts on zirconia particles and their application as supports of hybrid catalyst. Polymer International, 2015, 64, 804-810.	1.6	6
128	Spectroscopic Limited Practical Efficiency (SLPE) model for organometal halide perovskites solar cells evaluation. Organic Electronics, 2018, 59, 389-398.	1.4	6
129	Reversible Threeâ€Color Fluorescence Switching of an Organic Molecule in the Solid State via "Pump–Trigger―Optical Manipulation. Angewandte Chemie, 2022, 134, .	1.6	6
130	Synthesis, characterization, and photovoltaic properties of acceptor–donor–acceptor organic small molecules with different terminal electron-withdrawing groups. Journal of Materials Science, 2014, 49, 5279-5288.	1.7	5
131	Multifunctional polymer nanoparticles: ultra bright near-infrared fluorescence and strong magnetization and their biological applications. RSC Advances, 2016, 6, 65426-65433.	1.7	5
132	Recent advances in assembled AIEgens for image-guided anticancer therapy. Nanotechnology, 2021, 32, .	1.3	5
133	Reversible Photoswitching between Fluorescence and Room Temperature Phosphorescence by Manipulating Excited State Dynamics in Molecular Aggregates. Angewandte Chemie, 2022, 134, .	1.6	5
134	Synthesis, characterization, and photovoltaic properties of a solution-processable two-dimensional-conjugated organic small molecule containing a triphenylamine core. Journal of Materials Science, 2015, 50, 57-65.	1.7	4
135	Effect of annealing temperature on internal absorption, charge recombination and internal quantum efficiency of HC(NH2)2PbI3 perovskite solar cells. Organic Electronics, 2020, 77, 105508.	1.4	4
136	Plasmon-coupled Au-nanochain functionalized PEDOT:PSS for efficient mixed tin–lead iodide perovskite solar cells. Chemical Communications, 2022, 58, 1366-1369.	2.2	4
137	Discrete Platinum(II) Metallacycles with Inner- and Outer-Modified 9,10-Distyrylanthracene: Design, Self-Assembly, and Luminescence Properties. Inorganic Chemistry, 2022, 61, 7231-7237.	1.9	4
138	Visualization of Macrophase Separation and Transformation in Immiscible Polymer Blends. CCS Chemistry, 2023, 5, 718-728.	4.6	4
139	Intensity-dependent transient photocurrent of organic bulk heterojunction solar cells. Journal of the Korean Physical Society, 2017, 70, 177-183.	0.3	3
140	Frontispiece: Organic molecular aggregates: From aggregation structure to emission property. Aggregate, 2021, 2, e118.	5.2	3
141	Chloride treatment for highly efficient aqueous-processed CdTe nanocrystal-based hybrid solar cells. Journal of Materials Chemistry C, 2018, 6, 11156-11161.	2.7	2
142	Long-lasting photoluminescence quantum yield of cesium lead halide perovskite-type quantum dots. Frontiers of Chemical Science and Engineering, 2021, 15, 187-197.	2.3	2
143	Charge-carrier photogeneration and extraction dynamics of polymer solar cells probed by a transient photocurrent nearby the regime of the space charge-limited current. Frontiers of Chemical Science and Engineering, 2021, 15, 164-179.	2.3	2
144	Green-solvent-processed hybrid solar cells based on donor–acceptor conjugated polyelectrolyte. RSC Advances, 2018, 8, 38591-38597.	1.7	1

#	Article	IF	CITATIONS
145	Peptide-Conjugated Aggregation-Induced Emission Fluorogenic Probe for Glypican-3 Protein Detection and Hepatocellular Carcinoma Cells Imaging. Chemosensors, 2022, 10, 195.	1.8	1